UNIVERSITY OF VICTORIA

THE HUNT FOR DARK MATTER: WHY WE NEED TO UPGRADE THE SUPERKEKB

Thesis submitted to
the Department of Physics and Astronomy
in partial fulfillment of the requirements of
Physics 499

Winter Session 2019-2020
by

Karishma Moorthy
V00877081

Under the supervision of Dr. Michael Roney

Abstract

This thesis serves as a review of the Standard Model's weak mixing angle, and explores its application in the hunt for Weakly Interacting Massive Particles (WIMPs). Specifically, it looks at the departure of the weak mixing angle from theoretical expectation in the presence of intermediate-mass dark Z bosons, and compares it to the precision measurements possible (both present and projected) at the SuperKEKB, at the energy scale of the Belle II experiment ($Q = 10.58$ GeV). We find that the proposed upgrade of adding polarization to the electron beams, is required to be able to detect aforementioned discrepancies in the weak mixing angle at $Q = 10.58$GeV.

Acknowledgements

Contents

Natural units will be used throughout this thesis i.e. $\hbar = \mathrm{c} = 1$

The Hunt for Dark Matter:
Why we need to upgrade the SuperKEKB

Karishma M.

Winter Session 2019-2020

Under the supervision of Dr. Michael Roney

1 Introduction

1.1 Why WIMPs

Physicists have a very comprehensive theory to explain gravitational phenomena: The theory of General Relativity. This theory is well-tested and is yet to be disproven. The problem is, when you observe the movement of galaxies, things don't add up. Our theories predict that the galaxies are spinning too fast to not rip themselves apart. This was first analyzed by Vera Rubin in the 1960s and 70s. Many explanations were offered to explain this observation; one of which was that there was "invisible extra mass" which formed a sort of 'halo' around galaxies. This extra mass is what we call **dark matter**. There were many other anomalous observations made in subsequent years, many of which could be explained by the existence of dark matter.

Up until recently, there was a lot of debate around whether or not dark matter existed: what if our theories are just wrong? People proposed many alternate theories of gravity that built upon Newtonian dynamics (e.g. MONDs) and/or suggested that gravity could act non-locally etc. In 2006, images of the Bullet Cluster showed in great detail, that there was, in fact, extra matter that we could not see[1][3].

Though the existence of dark matter is generally accepted, its nature is highly contested [8]. Physicists have a very well-established and rigorously tested mega-theory that explains the nature of all the particles we observe today: it is called "the Standard Model"; it is based on the framework of Quantum Field Theory (QFT). Unfortunately, this model has nothing to say about dark matter [20]. All we really know about dark matter, through observation, is that it interacts via gravity, and does not interact via electromagnetism.

Presently, there are many hypotheses attempting to extend and/or supplement the Standard Model, to explain dark matter; One such (fairly popular) idea is that dark matter consists of Weakly Interacting Massive Particles (WIMPs). The popularity of the WIMP model does, in part, stem from the hope that WIMPs will also explain the positron excess observed in the Universe (for example, see Ref. [5])

For this project, we look at a WIMP model where it is assumed that dark matter also likely interacts via a weak interaction, through a dark Z boson Z_d, analogous to its Standard Model counterpart. Many attempts have been made to detect such WIMPs, and one such attempt is being proposed for the Belle II experiment. The Standard Model's Z boson exhibits a phenomenon called *parity* violation (as a result of the Weak Interaction[2]). Since a Z_d boson is analogous to the latter, it too should exhibit parity violation.

---

[1]Either that, or the gravitational lensing effect was a result of non-local gravity. But this "non-local gravity effect" is only observed in places where dark matter (if it exists) and ordinary matter would be separated by physical processes (e.g. colliding galaxy clusters). This effect isn't seen in galaxy clusters that aren't colliding: we see gravitational lensing effect right around the ordinary matter in those clusters (i.e. gravity effects are local there). There were also additional constraints added on by analysis of gravitational waves, which none of our current modified-gravity theories can explain. Hence, the majority of Physicists agree that dark matter is the cause for these anomalies [3]

[2]Only the Weak Interaction exhibits parity violation. This is because the 2 vertex factors of the Weak Interaction comprise of a vector component (and corresponding coupling) and axial vector component (and corresponding coupling). This is one of the results of the GWS model, seen in Figure 2. Because of this "V-A" structure, parity is not conserved in Weak interactions

The hope is to detect the indirect effects of this parity violation, and find it to be distinct from those predicted by the Standard Model, hence moving beyond the Standard Model.

1.2   Belle II at the SuperKEKB

The SuperKEKB is an electron-positron collider located in Japan. Its center-of-mass energy is around 10.58GeV , which is at the resonance of the B meson. Hence many, many B mesons are produced, and it is referred to as a "B factory"[1]. Presently, the electron and positron beams are unpolarized. We want to upgrade the SuperKEKB, to add polarization to the electron beam, so as to measure parity violations more precisely.

Measuring "parity violation" on its own is meaningless, if you cannot connect it to the Standard Model. The Weak Interaction, in the Standard Model, is described by several parameters... one of which is the weak mixing angle (See next Section). This is connected, by a fair bit of math, to the measurable asymmetries caused by parity violation[3]. Hence, to measure the parity violation experimentally, and compare it with the existing theoretical framework, the weak mixing angle is used (See Section 2.3).

Specifically, weak mixing angle measurements are made through measurements for forward-backward asymmetries and left-right asymmetries[4]. Forward-backward asymmetries can be measured right now at the SuperKEKB, and this can be used to measure the weak mixing angle. Left-right asymmetries, at present cannot be measured because the beams are unpolarized. By adding *polarization* to the electron beams, left-right asymmetries can also be measured, making measurements of the weak mixing angle more precise [2]. This is described, in more detail, in Section 2.4.

The weak mixing angle is fairly sensitive to new Physics, since we can make our measurements pretty precisely, and we can cross-check them with increasingly precise theoretical data [6][18]. The objective of this project is to develop the theoretical backing to help justify the potential upgrade, to introduce polarization to the electron beams, of the SuperKEKB. The main focus is on the dark boson masses (M_{Z_d}) implied by the potential measurements of mixing angle (made possible by the upgrade), made at the energy scales of the Belle II experiment.

2   Weak Interaction in the Standard Model

2.1   The Mathematical Framework of GWS model

In the early 1950s or so, the Fermi theory was the prevalent theory that explained the Weak Interaction. Roughly speaking, it explained the then observed instances of parity violation, via a weak interaction which involved the Fermi Constant G_μ[5]. This theory worked very well at low energies but broke down at high energies [24][14]. Around this time, neutrinos were discovered... but all the observed neutrinos were only left-handed (and their anti-particles were only right-handed). Based on the above facts, many theories were developed in the '60s and early '70s. Eventually in the late 1970s, the Glashow-Weinberg-Salam (GWS) model was found to be the winning theory, as confirmed by the measurement of the weak mixing angle, in experiments involving deep inelastic scattering of electrons on deuterium atoms [22][26]. The GWS model is a **non-***abelian* gauge theory; its basic recipe is outlined below:

1. We start off with the *assumption* that the universe began with left-handed electrons having $SU(2)$ symmetry, and with all fermions (i.e. **massless** electrons and neutrinos) having $U(1)$ symmetry i.e. We also *assume* that right-handed neutrinos do not exist.

2. For field Lagrangian to have said symmetry in the early universe, and continue to have a specific version of this symmetry now, we introduce gauge fields B_μ & $\vec{W}_\mu$, and quantum numbers: weak isospin (T), its third component (T_3) & weak hypercharge (Y).

3. We introduce a new complex scalar field ϕ (the Higgs field), such that:

---

[3] For this math, please see Ref. [2]. Here, only results from this paper will be quoted.
[4] See Ref. [2] for how these are measured.
[5] This was found through measurements of the lifetime of muon decays [24][14].

(a) When massless electrons interact with it, they gain the masses we observe

(b) When massless gauge bosons interact with it, we get massive $W^{\pm}$ & Z bosons, and a massless photon

(c) Therefore symmetry is spontaneously broken (hidden): $SU(2)_L \times U(1)_Y$ with all massless fermions $\rightarrow SU(2)_L \times U(1)_Y$ with some massive and some massless fermions[6], while the Higgs field reaches its vaccuum expectation value (v).

Refer Figure 1 for a more mathematically driven version of above recipe.

The results of this model are outlined in the Figure 2 seen below. As shown in the figure, one of the results that pops out of this model is **the weak mixing angle**: It will be the primary focus of this thesis.

---

[6]the GWS model does consider the neutrino to be massless, even though that is not true. This has been addressed in later models. Also, the exact mechanism by which the Higgs field is introduced and the symmetry is broken, is given in more recent models [19]. But all these models build upon the GWS model, hence the GWS model is still considered correct

a) Starting with Dirac Field Lagrangian: (used for all fermions)

$$\mathcal{L} = \bar{\nu}_e(x)\mathrm{i}\partial\!\!\!/\nu_e(x) + \bar{e}_\mathrm{L}(x)\mathrm{i}\partial\!\!\!/e_\mathrm{L}(x) + \bar{e}_\mathrm{R}(x)\mathrm{i}\partial\!\!\!/e_\mathrm{R}(x) \qquad \Psi(x) = \begin{pmatrix} \nu_e(x) \\ e_\mathrm{L}(x) \\ e_\mathrm{R}(x) \end{pmatrix}$$

⬇ Electron neutrino (left-handed) ⬇ Electron (left-handed) ⬇ Electron (right-handed)

Need U(1) symmetry:
$$\begin{pmatrix} \nu_e \\ e_\mathrm{L} \\ e_\mathrm{R} \end{pmatrix} \rightarrow \begin{pmatrix} \mathrm{e}^{-\frac{\mathrm{i}\beta(x)}{2}} & 0 & 0 \\ 0 & \mathrm{e}^{-\frac{\mathrm{i}\beta(x)}{2}} & 0 \\ 0 & 0 & \mathrm{e}^{-\mathrm{i}\beta(x)} \end{pmatrix} \begin{pmatrix} \nu_e \\ e_\mathrm{L} \\ e_\mathrm{R} \end{pmatrix}$$

and SU(2) symmetry:
$$\begin{pmatrix} \nu_e \\ e_\mathrm{L} \end{pmatrix} \rightarrow \mathrm{e}^{\frac{\mathrm{i}}{2}\boldsymbol{\tau}\cdot\boldsymbol{\alpha}(x)} \begin{pmatrix} \nu_e \\ e_\mathrm{L} \end{pmatrix} \qquad \text{while:} \qquad e_\mathrm{R} \rightarrow e_\mathrm{R}$$

where: $\boldsymbol{\tau} = (\tau_x, \tau_y, \tau_z)$ are the Pauli matrices and $\beta(x)$ & $\boldsymbol{\alpha}(x)$ are arbitrary scalar and vector functions respectively

b) Introduce the following:

and redefine:
$$\Psi = \begin{pmatrix} L \\ R \end{pmatrix}$$

where:
$$L = \begin{pmatrix} \nu_e \\ e_\mathrm{L} \end{pmatrix} \qquad R = e_\mathrm{R}$$

where, charge $Q = \mathrm{T}_3 + \dfrac{Y}{2}$

Field	ν_e	e_L	e_R
Y	-1	-1	-2

Table of weak hypercharge Y

Field	ν_e	e_L	e_R
T	$\frac{1}{2}$	$\frac{1}{2}$	0
T_3	$\frac{1}{2}$	$-\frac{1}{2}$	0

Table of isospin quantum numbers T_3 and T

and replace derivatives ∂_μ in the Lagrangian with covariant derivatives:

$$D_\mu L = \partial_\mu L - \frac{\mathrm{i}}{2}g\boldsymbol{\tau}\cdot\boldsymbol{W}_\mu L + \frac{\mathrm{i}}{2}g'B_\mu L, \qquad D_\mu R = \partial_\mu R + \mathrm{i}g'B_\mu R$$

Our resulting, locally symmetric, Lagrangian is given by

$$\mathcal{L} = R\mathrm{i}\gamma^\mu\left(\partial_\mu + \mathrm{i}g'B_\mu\right)R + L\mathrm{i}\gamma^\mu\left(\partial_\mu - \frac{\mathrm{i}}{2}g\boldsymbol{\tau}\cdot\boldsymbol{W}_\mu + \frac{\mathrm{i}}{2}g'B_\mu\right)L$$

$$-\frac{1}{4}\boldsymbol{G}_{\mu\nu}^{(W)}\cdot\boldsymbol{G}^{(W)\mu\nu} - \frac{1}{4}F_{\mu\nu}^{(B)}F^{(B)\mu\nu},$$

L = doublet
R = singlet

where $\boldsymbol{G}_{\mu\nu}^{(W)} = \partial_\mu \boldsymbol{W}_\nu - \partial_\nu \boldsymbol{W}_\mu + g\boldsymbol{W}_\mu \times \boldsymbol{W}_\nu$ and $F_{\mu\nu}^{(B)} = \partial_\mu B_\nu - \partial_\nu B_\mu$, $\boldsymbol{W}_\mu$ & B_μ

are the gauge fields for SU(2) and U(1) symmetry respectively, and g & g' are the 2 coupling constants of the (semi-unified) electroweak theory

c) Introduce the Higgs field:
$$\phi = \begin{pmatrix} \phi^+ \\ \phi^0 \end{pmatrix} = \frac{1}{\sqrt{2}}\begin{pmatrix} \phi_3 + \mathrm{i}\phi_4 \\ \phi_1 + \mathrm{i}\phi_2 \end{pmatrix}$$
which has: $Y = +1, \quad \mathrm{T} = 1/2$

Define covariant derivative: $D_\mu\phi = \partial_\mu\phi - \dfrac{\mathrm{i}}{2}g\boldsymbol{\tau}\cdot\boldsymbol{W}_\mu\phi - \dfrac{\mathrm{i}}{2}g'B_\mu\phi$

The Higgs field will give a contribution $\mathcal{L}_\phi$ to the Lagrangian of

$$\mathcal{L}_\phi = (D^\mu\phi)^\dagger(D_\mu\phi) + \frac{m_\mathrm{h}^2}{2}\phi^\dagger\phi - \frac{\lambda}{4}(\phi^\dagger\phi)^2$$

Final, pre-symmetry broken Lagrangian is given by: $\mathcal{L} + \mathcal{L}_\phi$

Figure 1: The recipe for the GWS model. Derived from Ref. [19]

Spontaneous symmetry breaking (hiding) occurs as Higgs field undergoes 2nd order transition to new ground state:

$$(\phi)_0 = \begin{pmatrix} \phi^+ \\ \phi^0 \end{pmatrix}_0 = \begin{pmatrix} 0 \\ v \end{pmatrix}$$

$$\Rightarrow \quad \phi = \begin{pmatrix} 0 \\ v + \frac{h(x)}{\sqrt{2}} \end{pmatrix}$$

This results in:

$$\mathbf{W}_\mu = (W_\mu^1, W_\mu^2, W_\mu^3)$$

$$W_\mu^\pm = \frac{1}{\sqrt{2}}(W_\mu^1 \mp i W_\mu^2)$$

and
— Z boson's field

$$\begin{pmatrix} Z_\mu \\ A_\mu \end{pmatrix} = \begin{pmatrix} \cos\theta_W & \sin\theta_W \\ -\sin\theta_W & \cos\theta_W \end{pmatrix} \begin{pmatrix} W_\mu^3 \\ B_\mu \end{pmatrix}$$

↑ Electromagnetic field

and all allowed interaction vertices:

where:

$$M_W^2 = g^2 v^2 / 2$$

$$M_e \neq 0$$

$$M_H = \lambda v = \sqrt{-2\mu^2}$$

$$|e| = g\sin\theta_W$$

$$M_Z = \frac{M_W}{\cos\theta_W}$$

NOTE: The symbol μ used in this image (and the previous one) is a parameter in the Higgs potential.
It will no longer be used to represent this parameter in forthcoming sections

Weinberg weak mixing angle:

$$\sin^2\theta_W = 1 - \frac{M_W^2}{M_Z^2} = \frac{g'^2}{g^2 + g'^2}$$

This is the definition used in the on-shell renormalization scheme (described in forth-coming sections) However, the idea of observable masses for unstable particles, becomes ambiguous at higher energies. So we sometimes instead use

This definition is used for the MS renormalization scheme. It requires that coupling constants be defined in as scale dependent quantities (explained in forth-coming sections)
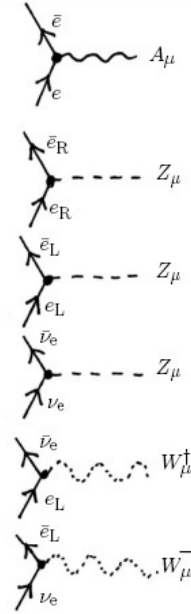
$$\frac{-ig}{2\sqrt{2}}\gamma^\mu(1 - \gamma^5) \quad (W^\pm \text{ vertex factor})$$

$$\frac{-ig'}{2}\gamma^\mu(v_f - a_f \gamma^5) \quad (Z^0 \text{ vertex factor})$$

with:

For Fermion f	Vector coupling v_f	Axial Vector coupling a_f
ν_e, ν_μ, ν_τ	$\frac{1}{2}$	$\frac{1}{2}$
e^-, μ^-, τ^-	$-\frac{1}{2} + 2\sin^2\theta_w$	$-\frac{1}{2}$
u, c, t	$\frac{1}{2} - \frac{4}{3}\sin^2\theta_w$	$\frac{1}{2}$
d, s, b	$-\frac{1}{2} + \frac{2}{3}\sin^2\theta_w$	$-\frac{1}{2}$

Figure 2: The summary of results of the GWS model. This was collected from Ref. [19], [14], [15] & [11]

2.2 Theory to Experiment: A QFT grab-bag

As alluded to in the previous Section, the Lagrangian of a theory gives rise to its coupling constants and allowed interactions i.e. the allowed *Feynman Diagrams*. The prescription required to go from Feynman diagram (derived from the theory) to the *cross-section*/decay rate (to be tested by experiment), is given by the **Feynman rules**: they are a systematic method to apply the tenants of Quantum Field Theory. There are senior-undergraduate Physics courses that cover this in detail. For a comprehensive explanation of the inner workings of this process, See Ref. [14], Chapter 6. The summarizing features of this chapter, and the concepts required to understand this thesis, are given in Figure 3, its caption and Table 1. Make sure to familiarize yourself with the table before moving forward.

p_1	$=$	4-momentum of input Particle A	
p_2	$=$	4-momentum of input Particle B (which, in other theories/diagrams, could also just be the anti-particle of A)	
p_3	$=$	4-momentum of output Particle A (which, in other theories/diagrams, could be some other particle/anti-particle)	see Figure 3
p_4	$=$	4-momentum of output Particle B (which, in other theories/diagrams, could be some other anti-particle/particle)	
t	$=$	$(p_1 - p_3)^2 = (p_4 - p_2)^2$	a *Mandelstam variable*
s	$=$	$(p_1 + p_2)^2 = (p_4 + p_3)^2$	a Mandelstam variable
E_{CM}	$=$	$\sqrt{s}$	Center of mass energy
q^2	$=$	t	$q^2 > 0 \rightarrow$ particle-antiparticle scattering; $q^2 < 0 \rightarrow$ particle-particle scattering as per most commonly used 4-vector convention where Minkowski metric $g_{\mu\nu} = 1, -1, 0$ for $\mu = \nu = 0$, $\mu = \nu \neq 0$, & $\mu \neq \nu$ respectively
q	$=$	4-momentum of virtual particle of tree diagram	used in scattering amplitude calculations; see Figure 3
k	$=$	4-momentum of virtual particle in loop	used in scattering amplitude calculations; see Figure 3
Q^2	$=$	$|q^2|$	Momentum transfer energy (squared) and y is a kinematic variable that represents the fact that experimentally, Q can be anywhere between 0 and the center of mass energy
	$=$	ys $\qquad\qquad 0 < y < 1$	
μ	$=$	Depends on circumstance	't Hooft scale; arbitrary mass parameter that falls out of dimensional regularization; often just referred to as 'scale'

Table 1: Energy Scales and 4-momenta: What the symbols mean

In QFT, anything that *can* happen, happens. Technically, all possible diagrams (i.e. sum[7] of all scattering amplitudes, $\mathcal{M}$) for a given interaction, contribute to the cross-section/decay rate. The math of the theory only decides the "importance" of each $\mathcal{M}_{i\epsilon[1, n \to \infty]}$. Often, some of the $\mathcal{M}$ are more important than others, for a given process (at a given energy): so here we neglect the $\mathcal{M}$'s in order of decreasing importance $\Longleftrightarrow$ process is **perturbative** (at that energy). If ALL the $\mathcal{M}$ are comparably important for a given process at a given energy, then your series diverges, and the process is **non-perturbative** at that

---

[7]The word 'sum' is used loosely here - things become complicated when dealing with spins and such. In practice, $\mathcal{M} = \mathcal{M}_1 \pm \mathcal{M}_2 \pm ....$ where $\pm$ depends on other more complicated aspects of the theory. See, for example, Ref. [14], Chapter 7
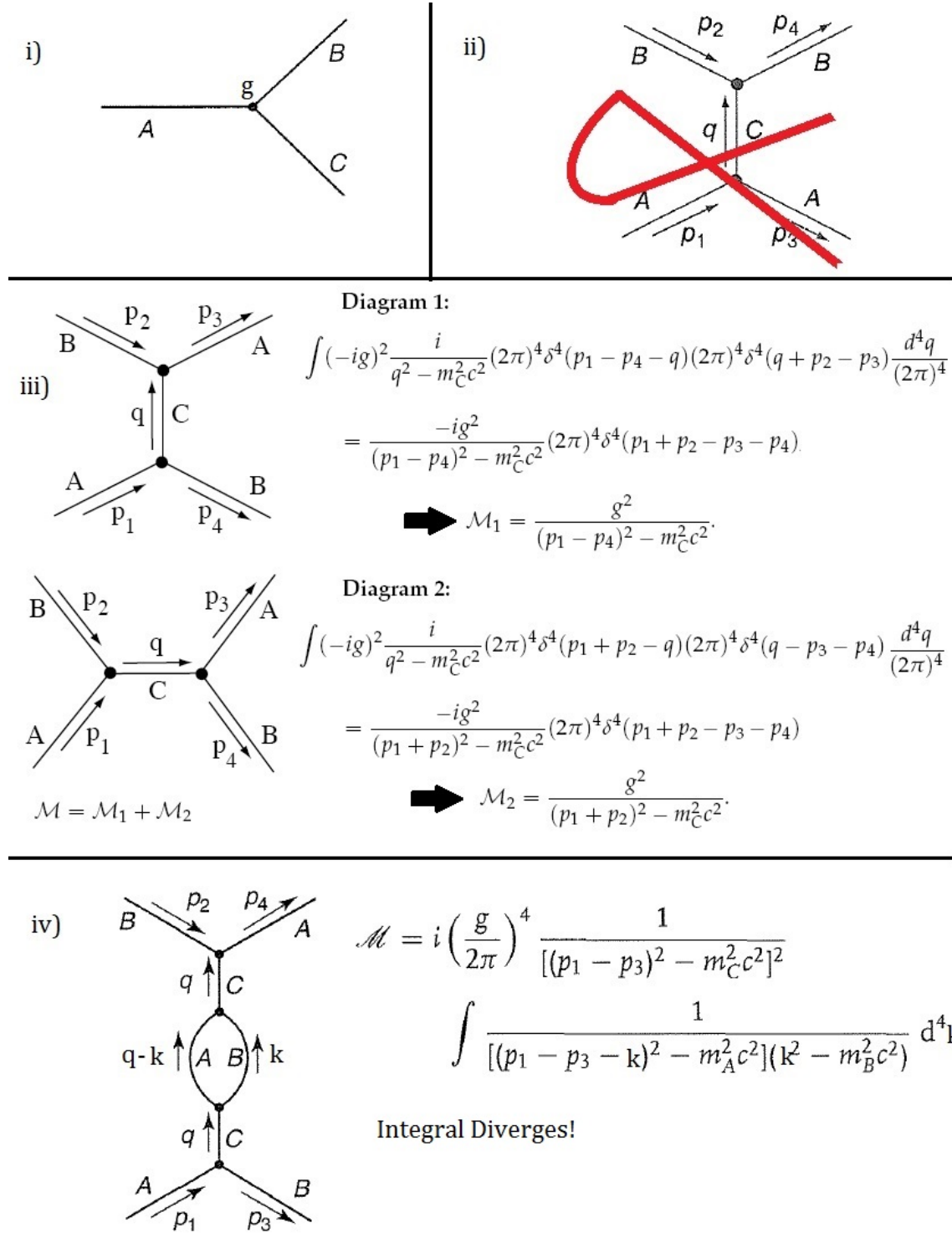
i)

ii)

iii)

Diagram 1:

$$\int (-ig)^2 \frac{i}{q^2 - m_C^2 c^2} (2\pi)^4 \delta^4(p_1 - p_4 - q)(2\pi)^4 \delta^4(q + p_2 - p_3)\frac{d^4 q}{(2\pi)^4}$$

$$= \frac{-ig^2}{(p_1 - p_4)^2 - m_C^2 c^2}(2\pi)^4 \delta^4(p_1 + p_2 - p_3 - p_4)$$

$$\Longrightarrow \mathcal{M}_1 = \frac{g^2}{(p_1 - p_4)^2 - m_C^2 c^2}.$$

Diagram 2:

$$\int (-ig)^2 \frac{i}{q^2 - m_C^2 c^2}(2\pi)^4 \delta^4(p_1 + p_2 - q)(2\pi)^4 \delta^4(q - p_3 - p_4)\frac{d^4 q}{(2\pi)^4}$$

$$= \frac{-ig^2}{(p_1 + p_2)^2 - m_C^2 c^2}(2\pi)^4 \delta^4(p_1 + p_2 - p_3 - p_4)$$

$$\Longrightarrow \mathcal{M}_2 = \frac{g^2}{(p_1 + p_2)^2 - m_C^2 c^2}.$$

$$\mathcal{M} = \mathcal{M}_1 + \mathcal{M}_2$$

iv)

$$\mathcal{M} = i\left(\frac{g}{2\pi}\right)^4 \frac{1}{[(p_1 - p_3)^2 - m_C^2 c^2]^2}$$

$$\int \frac{1}{[(p_1 - p_3 - k)^2 - m_A^2 c^2](k^2 - m_B^2 c^2)} d^4 k$$

Integral Diverges!

Figure 3: The ABC Toy model[*1], of spin-0, no-antiparticle particles: **Figure i)** shows the only allowed vertex $\Rightarrow$ decays of $A \to B + C$, $B \to A + C$ and $C \to B + A$ are allowed, but $A \to B + B$ and **Figure ii) is not allowed. Figure iii)** shows all the **tree-level** Feynman diagrams in the scattering process of $A + B \to A + B$. **Figure iv)** shows one possible 1-loop correction to Diagram 1 of Figure iii). The scattering amplitude $\mathcal{M}$[*1] here, **diverges**. This is different from that of Figure iii), which gives a definitive expression for $\mathcal{M}$. [Figure has been adapted from [14] and its solution manual]

[*1] For a more realistic model, see Chapter 7 of Ref. [14]

[*2] $\mathcal{M}$ is a quantity directly used in finding the cross-section for a scattering process

energy. Generally speaking, perturbative processes are easier to calculate than non-perturbative ones. Most simple[8] QED interactions are perturbative at their respective energy scales. QCD interactions at higher energy scales ($> \sim 0.1\text{GeV}$[9]) are typically perturbative. QCD interactions at lower energy scales, however, are non-perturbative.

For the moment, let us consider a perturbative interaction i.e. there are a finite number of Feynman diagrams that contribute to it (a finite number of "important ones"). As seen in Figure 3, higher-order loop diagrams lead to scattering amplitudes that involve diverging integrals. The problem arises because, technically, k can take any value in the d^4k space and the diagram is still possible: q does not constrain k enough. To solve the problem and get a physically-consistent cross-section, we need to **regularize** this integral and then **renormalize** the masses and coupling strengths.

Roughly speaking, regularization introduces a new regularization parameter i.e. "cut-off scale", Λ, to the scattering amplitude, such that:

$$\Lambda \to \infty \Rightarrow \mathscr{M}(..,..,..,\Lambda) \to \mathscr{M}(..,..,..)$$

This regularization parameter is introduced so that all divergences of the integral (in $\mathscr{M}$) appear as singularities in the parameter (Λ) [17].

Conceptually, Λ can be thought of as a means to constrain the range of values k can take. When $\Lambda \to \infty$ k has its full range available to it $\Rightarrow$ the integral diverges. But Λ is typically chosen to be finite (so that $\mathscr{M}$ is defined). We can make this choice, because we are *assuming* that k^2 is more likely to NOT be much greater than q^2,[10]... so for Λ greater than, but in the order of q^2, $\ln \frac{k^2}{\Lambda^2}$ is likely negligible and can be cancelled out.

Depending on the regularization scheme, the integrals are seen to diverge with Λ^2 or $\ln \Lambda$ for $\Lambda \to \infty$ (or to have poles in powers of ε, for $\varepsilon \to 0$, in dimensional regularization, explained below). These divergences can be removed by working with renormalized fields, mass, and coupling constants right from the beginning[17]. To do this, you redefine the coupling constants (say, g) and masses (say m), such that:

$$g_R(q^2) := f(q^2, g, \mu, m_R(q^2))$$

$$m_R(q^2) := h(q^2, m, \mu, g_R(q^2))$$

where, f and h are functions that need to be found through renormalization, μ is the **renormalization scale**[11] and the subscript R is used for renormalized quantities. g & m are **bare parameters**, that *represent* the coupling constant and mass respectively - but on their own, they are physically meaningless. Yes, the parameters of the Lagrangian are actually not defined in value; they can never be measured! Only g_R and m_R can be measured... and they will have different FINITE values for different FINITE q and μ values. This phenomenon is called **running**. Note that $g_R(q^2)$ and $m_R(q^2)$ form a coupled system of equations $\to$ hence it *requires* that $g_R(q^2 = q_0^2)$ and $m_R(q^2 = q_0^2)$ for some q_0, be measured *experimentally*. This is why there are so many free parameters in the Standard Model that need to be measured, to be able to make the predictions it does.

m_R will no longer be used to denote renormalized masses; Henceforth, M will be used to denote renormalized masses, and m to denote bare masses.

In practice, there are many ways to perform said renormalization. Different renormalization schemes, have different ways of removing the infinities of Λ (*or* poles of ε), which leads to different cross-section formulae. We expect (if nothing went wrong) that each of these renormalization schemes are equivalent to each other at the same order, leading to the same measurable quantity. The uncertainty in the expected value of the measurable quantity, is what is referred to as the **theoretical uncertainty**

---

[8]The interactions of/by the Hydrogen atom, for example, are not "simple". In senior undergraduate Quantum Mechanics courses, one does perturb the ground state of the Hydrogen atom to derive other results... but the ground state of the Hydrogen atom itself is non-perturbative.

[9]i.e. around the lightest hadron mass scale

[10]For very very large q^2, the theory does break down. "How large?" is a question that is answered by the specifics of the problem at hand.

[11]This is different from Λ. How it works depends on the renormalization scheme used.

of the problem. Theoretical uncertainty exists because of the inadequacies in our methods that prevent us from getting an exact answer: Different renormalization schemes have different strengths/inadequacies.

In this thesis, 2 popular renormalization schemes are explored: the on-shell renormalization scheme and the $\overline{MS}$ scheme[12]. Both of these renormalization schemes require that you regularize the divergences using **dimensional regularization**. This is a popular method of regularization, championed by 't Hooft in the early 70s[16], and it is the only one employed in this thesis.

In dimensional regularization, the "cut-off" is given by $\varepsilon = D - 4$. Here, the d^4k integral is taken to a lower dimension D, where the integral converges. This procedure is Lorentz and gauge invariant[15]. To do this, and still maintain the dimensions of the integral, the 't Hooft scale, μ had to be introduced as so:

$$\int (...) \frac{d^4k}{(2\pi)^4} \to \mu^{-\varepsilon} \int (...) \frac{d^D k}{(2\pi)^D}$$

The contents within the parentheses are also made dimensionless using μ, since μ has the dimensions of mass[13]. As part of dimensional regularization, the expression is then perturbatively expanded as a Laurent expansion[14] of sorts, where the residues are functions of the bare parameters $\& \mu$, and for poles at $\varepsilon \to 0$. For all integrals that can occur in the perturbation expansion of the above expression, one can define in a unique way its finite part as an analytic function of D [16]. All the divergences of the integral manifest themselves as singularities of the type $1/\varepsilon_j, j = 1, 2, 3, ...L$, where L is the number of loops in the Feynman diagram this integral represents[17]. These analytic functions are then systematically simplified, through fairly advanced mathematics.

Then, as part of the renormalization (whichever scheme it is), bare parameters are written as function (or rather, a kind of infinite sum of functions of) their respective renormalized parameters, at a specific choice of scale μ, where the μ is used to decide which terms are "negligible" in the perturbative expansions described above. Eventually, $\epsilon \to 0$, i.e. D $\to$ 4, to give an expression for finite physical (renormalized) quantities, dependent on μ[15].[16]

For a complete explanation of the topics touched upon above, please refer to Ref. [14], [19] [15], [17] and [16]. Ref. [15] is a good explanation for the on-shell renormalization scheme, applied in the context of the weak mixing angle. Ref. [17] contains an especially good, and rigorous explanation for dimensional regularization and the $\overline{MS}$ renormalization scheme applied to ϕ^4 theories (the GWS model is a ϕ^4 theory - see Section 2.1). In Section 2.3, the results of the $\overline{MS}$ scheme, applied to the weak mixing angle, will be explained in further detail.

2.3   Running of the Weak Mixing Angle

In this section, I plot the running of the weak mixing angle from 10^{-4}-10^4GeV. In the previous section, we saw that renormalization naturally implies the running of physical quantities: I use 2 different implementations of the $\overline{MS}$ scheme (described further below), which replicate 'Figure 1' published in Ref. [18] and seems to be used in Ref. [9] for the dark Z boson mixing calculations. This will then be connected back to forward-backward and left-right asymmetries in Section 2.4, thus illustrating the theoretical uncertainty in the measurement of the weak mixing angle, as is relevant to the Belle II experiment.

From Ref.[13] and Ref.[7], we define:

---

[12]The exact derivation of the expressions used, is beyond the scope of this thesis. However, all the expressions used to get the results, will be quoted and supplemented with explanations of the basic features and motivations.

[13]In 't Hooft's original work, it was referred to as a "unit of mass"[16].

[14]A Laurent expansion of a function is equivalent to its Taylor expansion, when it is analytic at every point within its radius of convergence. Else, it will have poles and residues which are typically calculated through complex analysis. This is typically covered in senior undergraduate Mathematics courses. A good reference for this is Ref. [4].

[15]Exactly how it depends on μ, and how μ is used to remove the infinities, depends on the renormalization scheme chosen.

[16]The choice of μ is usually dependent on, and often interchangeable with, Q; see, for example, Ref. [10].

$$\sin^2 \theta_w(Q^2) := \kappa(Q^2)_{(on-shell)} \sin^2 \theta_{w(on-shell)} = \hat{\kappa}(Q^2, \mu) \sin^2 \hat{\theta_w}(\mu) \tag{1}$$

where,

$\hat{o} =$ 'o' is any quantity that pertains to/is derived from the $\overline{MS}$ renormalization scheme (this is notation that will be used throughout this thesis, and is found in many other papers/review articles as well).

$\sin^2 \hat{\theta_w}(\mu) =$ Scale dependent weak mixing angle, given by the $\overline{MS}$ scheme. The expression for this can be found here: Ref.[10], Eqn. 25. It is quoted below:

$$\sin^2 \hat{\theta_w}(\mu) = \frac{\hat{\alpha}(\mu)}{\hat{\alpha}(\mu_0)} \sin^2 \hat{\theta_w}(\mu_0) + \lambda_1 [1 - \frac{\hat{\alpha}(\mu)}{\hat{\alpha}(\mu_0)}] + \frac{\alpha(\mu)}{\pi} [\frac{\lambda_2}{3} \ln \frac{\mu^2}{\mu_0^2} +$$
$$\frac{3\lambda_3}{4} \ln \frac{\hat{\alpha}(\mu)}{\hat{\alpha}(\mu_0)} + \sigma(\tilde{\mu}_0) - \sigma(\tilde{\mu})] \tag{2}$$

where μ_0 is the particle mass threshold[17] nearest to μ, $\lambda_{1,2,3}$ are numerical coefficients that take on different values, depending on the scale ranging from μ_0 to μ, α is the (scale-dependent) fine structure constant and $\tilde{\sigma}$ is the (scale-dependent) QCD-related coefficient. It encodes tree-level asymmetry, QED and lowest-order QCD corrections. This expression is not useful at $\mu = \mu_0$. At particle mass thresholds, one must use a different renormalization scheme and/or directly use a measured value (from (1)).[18]

The value for the weak mixing angle, measured via the $\overline{MS}$ renormalization scheme, at the Z pole [12] is:

$$\sin^2 \hat{\theta_w}(\mu = M_z) = 0.23122 \pm 0.00003^{19} \tag{3}$$

$\hat{\kappa} =$ Form factor obtained from $\overline{MS}$ renormalization scheme. It encodes radiative corrections that are logarithmically-enhanced and/or cannot be accounted for, by (2); e.g. anapole moment[20] corrections or higher-order QCD corrections [10]. It is a purely theoretical quantity that is an artifact of aforementioned renormalization scheme.

$\sin^2 \theta_{w(on-shell)} =$ Weak mixing angle defined by:

$$\sin^2 \theta_{w(on-shell)} = 1 - \frac{M_w^2}{M_z^2} \tag{4}$$

where M_w and M_z are the renormalized masses (and therefore, the masses which can be measured) of the $W^{\pm}$ and Z^0 boson. It is a direct measure of tree-level asymmetry of the Weak Interaction. In practice, M_w is calculated using (4), and $\sin^2 \theta_{w(on-shell)}$ is calculated using M_z, $\hat{\alpha}(M_z)$ (fine structure constant measured at the Z pole) & G_μ (Fermi constant), treated as known (observed) values, and $M_{Higgs.boson}$ & $M_{top.quark}$ treated as contested (but still known) observed parameters ([12], Pg. 5-6). This is the case for us as well: See (12)

The value for the weak mixing angle, measured via the on-shell renormalization scheme, at the Z pole [12] is:

$$\sin^2 \theta_{w(on-shell)} = 0.22343 \pm 0.00007 \tag{5}$$

---

[17]These are colloquially called "particle masses" i.e. the renormalized mass values one would find, if one simply looked up the mass of each of the existing particles.

[18]For a good diagram of this scale dependence and measurements of it, please see Ref. [11], Fig. 1.

[19]$\sin^2 \hat{\theta_w}(\mu = M_z) = 0.23124(6)$ is used to obtain the continuous graph found in Ref.[9] and Ref.[18], from 2015 and 2013 respectively. As of 2019 however, the Particle Data Group (Ref.[12]) has documented that there still exists tension between measured values at the Z pole, despite it being our most precise measurement as yet. This consequently adds to the theoretical uncertainty in expected values in other energy scales. I have used the most recent value in my code, but have **not** accounted for this uncertainty.

[20]The Anapole Moment is a quantity pertaining to the electron. It is not a physical observable, and suffers from electroweak gauge ambiguities, but it does contribute to parity violation. See Appendix B of Ref. [6].

κ = Amplitude obtained from the on-shell renormalization scheme.[21] It is a purely theoretical quantity that is an artifact of aforementioned renormalization scheme - its expression depends on how many corrections are incorporated.[22] In our thesis, which is based heavily on Ref. [2], where κ encodes one-loop radiative corrections (including anapole moments) (See Section 3).

And $\sin^2 \theta_w(Q^2)$ is the running weak mixing angle. It is this quantity that is measured through experiment, at experiment-specific energy Q.[23]

(Please refer to table 1 for definitions of Q and μ)

Let us look further into what the specific expressions for the R.H.S. of (1) are and how they behave:

2.3.1   Implementation 1: The Gauge-dependent $\overline{MS}$ scheme

$$\hat{\kappa}(Q^2, \mu) \sin^2 \hat{\theta}_w(\mu) \qquad\qquad Q^2 \text{ around } M_z^2$$

$$= \hat{\kappa}(Q^2, \mu = M_z) \sin^2 \hat{\theta}_w(\mu = M_z)$$

(since the product doesn't depend on μ, μ can be chosen to be a specific value that is easy for us to work with. Since the weak mixing angle has been most extensively measured around the Z pole $\rightarrow$)

$$= \hat{K}(Q^2) \times <\text{value in (3)}>$$

$\hat{K}(Q^2)$ encodes ALL[24] one-loop radiative corrections to the tree-level asymmetry: the largest of these, are the WW box diagrams, the photonic vertex diagrams & box diagrams, γZ mixing and the anapole moment [7]. See Figure 4.

Unless stated otherwise, all expressions below (for the rest of Section 2.3.1) were obtained/inferred from the works of Czarnecki and Marciano (Ref.[7] & [6]) from the late 90s/early 2000s.

This is given by:

$$\hat{K}(Q^2) = \hat{K}_f(Q^2) + \hat{K}_b(Q^2) - 1 \tag{6}$$

where $\hat{K}_f(Q^2)$ encodes the radiative corrections due to the fermionic loops and $\hat{K}_b(Q^2)$ encodes the radiative corrections due to the bosonic loops.
$\hat{K}_f(Q^2) \rightarrow 1, \Rightarrow$ no contribution from fermion loops, to radiative corrections.
Similarly, $\hat{K}_b(Q^2) \rightarrow 1, \Rightarrow$ no contribution from boson loops
and $\hat{K}(Q^2) \rightarrow 1, \Rightarrow$ no one-loop radiative corrections.

---

[21] The expression for this has not been used in this thesis.

[22] In many places (example, by PDG), this is referred to as κ_f, where f refers to the fermions involved.
$\kappa_f \sim 1 + \frac{<another-fermion-dependent-form-factor-\rho_f>}{tan^2\theta_w(on-shell)}$ [12]. Also, typically, κ_f is used, when $\sin^2\theta_w(Q^2)$ refers to $\sin^2\theta_w(Q^2)^{eff}$ for low Q^2.
However, notation in this regard is generally used inconsistently in the literature. κ_f will not be used further in this thesis, to avoid confusion.

[23] For those familiar with the LEP convention of measuring weak mixing angle, $\sin^2\theta_w(Q^2) = (\hat{k}^{(e,e)}(Q^2, \mu = M_z) - 0.0044)\sin^2\theta_{w;eff}^{LEP}$ where $\hat{k}^{(e,e)}(Q^2, \mu = M_z)$ is BEFORE the correction (10) (read ahead for it), and the -0.0044 comes from the decay amplitude of an on-shell Z boson into a $l - \bar{l}$ pair [13].

[24] all, as opposed to just the anapole moment and the higher order QCD corrections. Hence the relabelling from $\hat{\kappa}$ (of (1)) to $\hat{K}$. But it should be noted that in most references, either $\hat{\kappa}$ or κ is used for this "mass-dependent" form factor. Be wary of such notational inconsistencies in the literature.
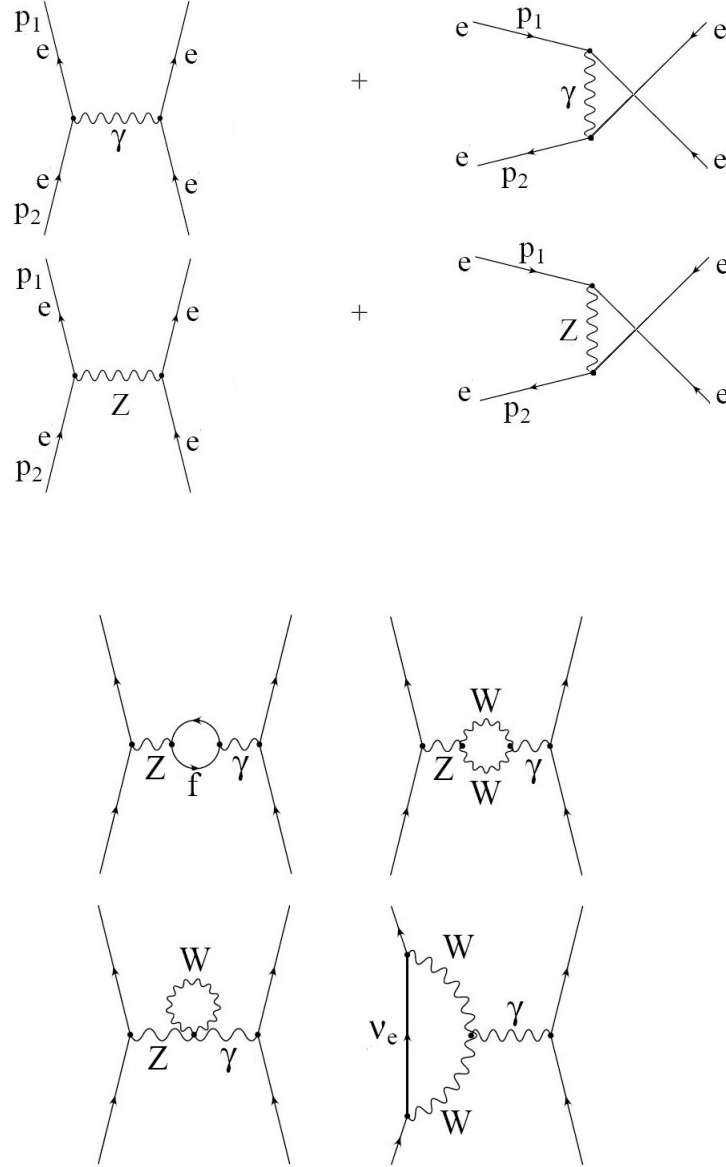
Figure 4: This is a sample of Feynman diagrams involved in finding the cross-section for the weak mixing angle, up-to one-loop radiative corrections. **Figure a)** shows Neutral currents direct and crossed e^-e^+ scattering amplitude leading to A_{LR} asymmetry at tree-level. **Figure b)** shows Photon Z mixing and W loop contributions to the anapole moment (Diagrams from [7] edited to show e^-e^+ rather than e^-e^- scattering)

$$\hat{K}_f(Q^2) = 1 - \frac{\alpha}{2\pi\hat{s}^2}\frac{N_c}{3}\sum_{all\,fermions,f}[(T_{3f}Q_f - 2\hat{s}^2)$$

$$(\ln\frac{M_f^2}{M_Z^2} - \frac{5}{3} + 4z_f + (1 - 2z_f)p_f\ln\frac{p_f + 1}{p_f - 1})]$$

(7)

$$z_f := \frac{M_f^2}{Q^2}$$

$$p_f := \sqrt{1 + 4z_f}$$

and

$$\hat{K}_b(Q^2) = 1 - \frac{\alpha}{2\pi\hat{s}^2}[-\frac{42\hat{c}^2 + 1}{12}\ln(\hat{c}^2) + \frac{1}{18}$$

$$-(\frac{p}{2}\ln\frac{p + 1}{p - 1} - 1)[(7 - 4z)\hat{c}^2 + \frac{1}{6}(1 + 4z)]$$

(8)

$$-z[\frac{3}{4} - z + (z - \frac{3}{2})p\ln\frac{p + 1}{p - 1} + z(2 - z)\ln^2\frac{p + 1}{p - 1}]]$$

$$z := \frac{M_W^2}{Q^2}$$

$$p := \sqrt{1 + 4z_f}$$

where,

N_c = No. of distinct colours fermion 'f' can have

T_{3f} = weak isospin of fermion 'f' = $\pm\frac{1}{2}$ (sign depending on the fermion 'f')

Q_f = electric charge of the fermion 'f'

$\hat{s}^2 = 1 - \hat{c}^2 = \sin^2\hat{\theta}_w(\mu = M_z) = \ <value\ in\ (3)>$

Note: These expression yields divergences in the low-energy regime, due to the logarithmic terms. This is seen in graph Figure 5. Just as a reminder: (6)(7)(8) are all based around the Z-pole; Hence it makes sense that $\hat{K}_b(Q^2)$ and $\hat{K}_f(Q^2)$ break down at low energies.

$\hat{K}(Q^2)$ is process independent but (electroweak) gauge-dependent [13]. At first, this seems problematic... after all, a gauge is just a mathematical "switch" of sorts; it should not affect measurable quantities: Physics must be gauge invariant. However, the effects of $\hat{K}(Q^2)$ are never directly measured. Only asymmetry is measured here. Typically, there are other components, in a measured quantity, calculated through similar means (for LR-asymmetry, for example, it is the other radiative corrections, $\Delta r \& \kappa$, in (12)(1) & (13)) that are also gauge-dependent: therefore the gauge dependencies cancel out and the measured quantity is gauge-invariant [10].

2.3.2 Implementation 2: The Process-dependent $\overline{MS}$ scheme

$$\hat{\kappa}(Q^2, \mu) \sin^2 \hat{\theta}_w(\mu) \qquad\qquad\qquad \text{Q}^2 << M_w^2$$

$$= \hat{\kappa}^{(e,e)}(Q^2, \mu) \sin^2 \hat{\theta}_w(\mu)$$

(For low energies, it is near impossible to work with the $\overline{MS}$ scheme AND include all the precision corrections we require, without choosing a specific interaction for which we can measure an asymmetry. The process we use here is e-e scattering. For Moller scattering $e^- e^-$, $Q^2 = -q^2$ and for Bhabha $e^- e^+$, $Q^2 = q^2$. Again, since the product doesn't depend on μ, we can choose $\mu = M_z \rightarrow$)

$$= \hat{\kappa}^{(e,e)}(Q^2, \mu = M_z) \times <\text{value in (3)}>$$

From the works of Ferroglia, Ossola & Sirlin, Ref. [13], Eqn. 5, 6 set to $\mu = M_z \Rightarrow$:

$$\hat{\kappa}^{(e,e)}(Q^2, \mu) = 1 + \frac{\alpha}{2\pi \hat{s}^2}[-2N_c \sum_{allfermions, f} [(T_{3f}Q_f - 2\hat{s}^2)I_f(Q^2)]$$

$$+ (\frac{7}{2}\hat{c}^2 + \frac{1}{12}) \ln \frac{M_w^2}{M_z^2} - \frac{23}{18} + \frac{\hat{s}^2}{3}] \qquad (9)$$

$$I_f(Q^2) = \int_0^1 dx\, x(1-x) \ln \frac{M_f^2 - Q^2 x(1-x)}{M_z^2}$$

where all the symbols are the same as the ones used in (7) & (8). Also, it should be noted that $\hat{\kappa}^{(e,e)}(Q^2, \mu = M_z)$ breaks down at $Q^2 = M_z^2$. There are no obvious divergences, but it is not supposed to work there and hence gives the wrong effective weak mixing angle at that energy.

As stated before, $\hat{\kappa}^{(e,e)}$ is process-dependent, but both $\hat{\kappa}^{(e,e)}(Q^2, \mu)$ and $\sin^2 \hat{\theta}_w(\mu)$ are gauge-independent [13]. And unlike K, which is constructed around $\mu = M_z$, $\hat{\kappa}^{(e,e)}$ is constructed with the assumption that $Q^2 << M_w$... and the choice of $\mu = M_z$, was merely for convenience. K and $\hat{\kappa}^{(e,e)}$ are fundamentally different expressions... they merely used the same renormalization scheme.

2.3.3 Combining the 2 implementations of the $\overline{MS}$ scheme

As explained in Section 2.3.1, having the final $\sin^2 \theta_w(Q^2)$ value be gauge-dependent is acceptable here. Since the goal is to replicate the graphs found in [18] and [9], where the effective running of the weak mixing angle is plotted independent of HOW it is measured (as it should be), the final expression used must be process-independent. Knowing that (6) and (9) each partially satisfy these conditions, we add the following correction to (9):

$$\hat{\kappa}^{(e,e)}(Q^2, \mu) \rightarrow \hat{\kappa}^{(e,e)}(Q^2, \mu) + \frac{\hat{\alpha}(M_z)}{4\pi \hat{s}^2} \qquad (10)$$

By doing this, (9) now matches up with the gauge choice[25] used to obtain (6)(7)(8)... and at all Q_0 common to both their ranges:

$$\hat{K}(Q_0^2) = \hat{\kappa}^{(e,e)}(Q_0^2, \mu) + \frac{\hat{\alpha}(M_z)}{4\pi \hat{s}^2} \qquad (11)$$

---

[25]Czarnecki and Marciano appear to have used the 't Hooft Feynman gauge to obtain $K(Q^2)$, and to incorporate WW box-diagrams and such into $\hat{\kappa}^{(e,e)}(Q^2, \mu)$ using that gauge, rather than assuming the process itself accounts for it, the correction is required [13].
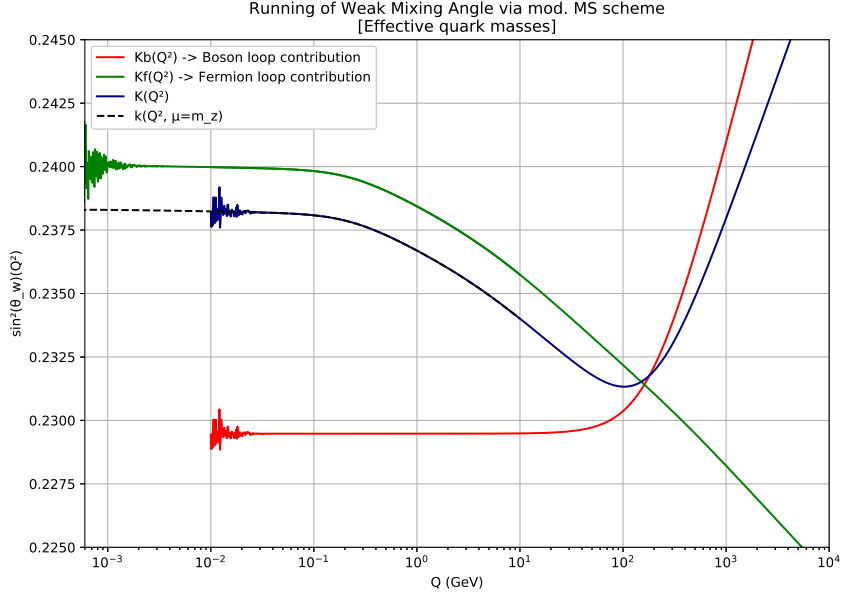
Figure 5: This is an illustration of the form factors from the different schemes used for our plots (all form factors appear as factors multiplying $\hat{s}^2$). Note how $\hat{K}_b(Q^2)$ and $\hat{K}_f(Q^2)$ become unstable at lower energies, which leads to $\sin^2\theta_w(Q^2)$ given by the $\hat{K}(Q^2)$, to become unstable at low energies... hence the requirement of corrected $\hat{\kappa}^{(e,e)}(Q^2, \mu = M_z)$ from (10). This is also meant to replicate Fig. 2 of Ref. [18]

Finally our expression meets our criteria - it is plotted in Figure 5, with an analysis of the origins of theoretical uncertainty explained below.

2.3.4 Points of note regarding Theoretical Uncertainty

1. In (7) and (9), masses of up, down and strange quarks are set to 0.1 GeV. This is to match the QCD corrections suggested by Marciano & Sirlin in 1982 (Ref. [21]). In general, QCD corrections are non-perturbative and therefore very difficult, if not impossible, to work with theoretically. A fair bit of study has gone into different ways of approximating/calculating these corrections, at different energy scales. For our purposes, it is adequate to analyze data from experiments based on similar Feynman diagrams, and empirically choose "effective quark masses", so that our expression fits the data. One can rationalize this choice by arguing that quarks cannot be found alone, hence considering them collectively "makes sense". Regardless, the choice of these *effective quark masses*, led to $\sin^2\theta_w(Q^2 = 0) = \sim 0.2383$, which is consistent with Fig. 1 of Ref. [9] and also [13] after correction of (10) is applied. This (with no scaling) is curve 6 in Figure 6.

2. According to Pg. 35 Ref. [18], experimentally:

$$\frac{N_c}{3} \sum_{allquarks,q} (T_{3q}Q_q - 2\hat{s}^2) \ln \frac{M_q^2}{M_Z^2} \to -6.88 \pm 0.06$$

Now, doing this rigorously requires "QCD dressing" of (6) and (9), which is beyond the scope of this thesis. It seems that Ref. [18] did this rigorously and that is why their $\sin^2\theta_w(Q^2 = 0) = \sim 0.2387$. Using the effective quark masses leads to a "quark sum" of ~ -6.52. Since both the quark sum, and the effective quark masses are, in essence, experimentally determined, they are both equally important. So to achieve *quark sum* of Ref. [18], I arbitrarily chose to set the masses of up, down and strange quarks to 0.06 GeV. This (with no scaling) is curve 4 in Figure 6.

15

3. Since $\sin^2 \theta_w (\mu = M_z)$ has to be measured directly, by (1), we expect $\hat{K}(Q^2 = M_z^2) = 1$. But in practice, it is near 1, but not exactly 1. This is understandable, since there is disagreement about the Z pole value of $\sin^2 \theta_w$ [12] - it must be taken into account. Hence I have plotted the "scaled versions"[26] of 1, 4 and 6 as curves 2, 5 and 7 respectively.

4. For the sake of illustrative purposes, I have also plotted how the curves look when you plug in our present measurements of free quark masses, given in the PDG [12]. $\sin^2 \theta_w (Q^2 = 0)$ here does not correspond to any measured or plotted value I could find. This is curve 1 in Figure 6. Also, just to demonstrate the effect of (10), I have plotted the uncorrected curves 3, 8 and 9 that correspond to 1, 4 and 6 respectively. **Both the no-quark-mass-correction and the uncorrected curves, will not be counted in theoretical uncertainty calculations**.

---

[26]By scaled version, I mean that for curves 1, 4 and 6, I divided them by the value of their respective form-factors at $Q^2 = M_z$. This is so that they will have exactly the value of $\sin^2 \theta_w (\mu = M_z)$ at $Q^2 = M_z$
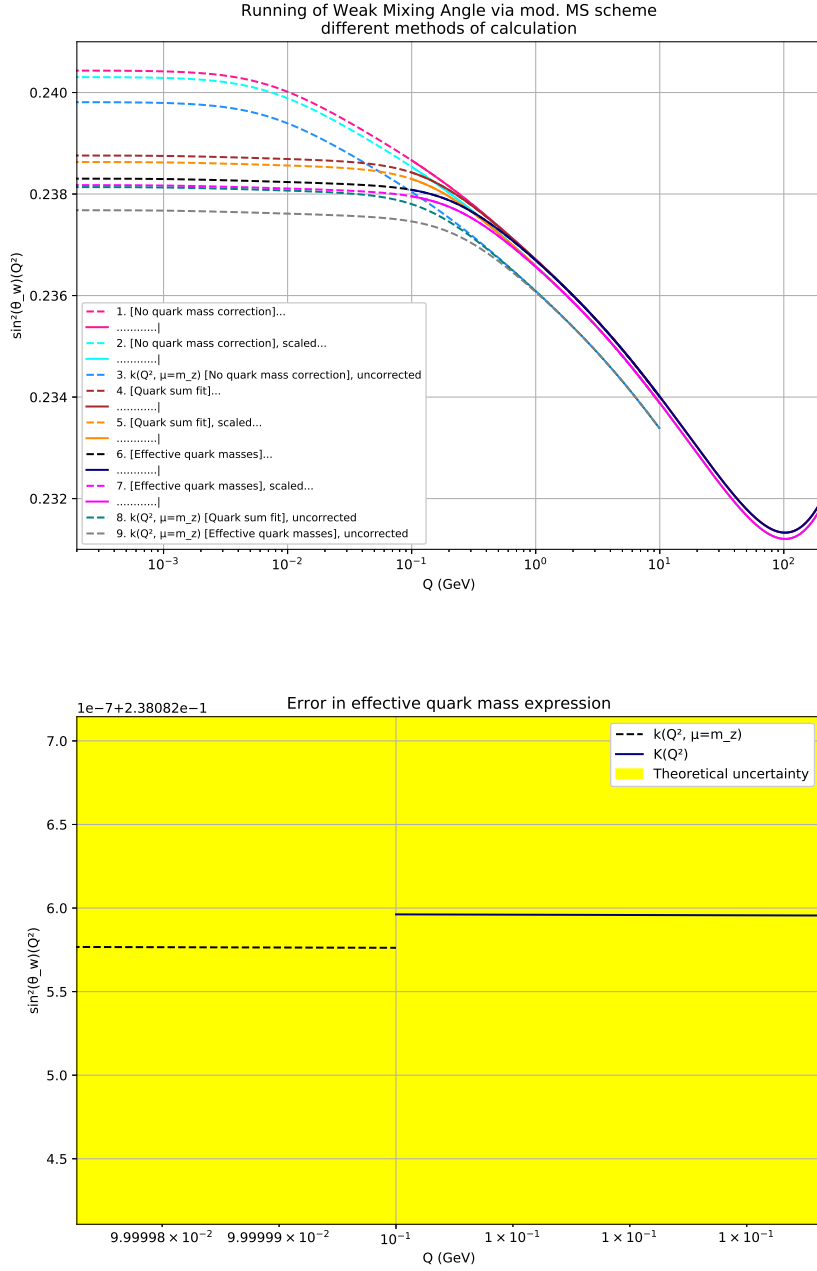
Running of Weak Mixing Angle via mod. MS scheme
different methods of calculation

1. [No quark mass correction]...
............|
2. [No quark mass correction], scaled...
............|
3. k(Q², μ=m_z) [No quark mass correction], uncorrected
4. [Quark sum fit]...
............|
5. [Quark sum fit], scaled...
............|
6. [Effective quark masses]...
............|
7. [Effective quark masses], scaled...
............|
8. k(Q², μ=m_z) [Quark sum fit], uncorrected
9. k(Q², μ=m_z) [Effective quark masses], uncorrected

Error in effective quark mass expression

k(Q², μ=m_z)
K(Q²)
Theoretical uncertainty

Figure 6: **Figure a)** Illustrates the results of using different scaling and quark masses. Please refer to the text for explanation The curves are numbered in the order they appear on the graph. Theoretical uncertainty is given by space between curve 4 and curve 7. Curve 6 is what is used for the values of the theoretical predictions for the weak mixing angle, henceforth. Note that the difference between the curves reduce significantly at higher energies. This eventually leads to an asymmetry in theoretical uncertainty (See Figure 7 and 12). **Figure b)** shows the discontinuity in Figure a)'s curve 6. This discontinuity is due to the fact that despite the correction in (11), the 2 different expressions do not merge exactly. I chose $Q_0 = 10^{-1}$GeV as the merging point by visually determining the region in which is discontinuity is minimized. Since this error is fairly insignificant when compared to the theoretical uncertainty, **curve 6 has been manually corrected (in addition to (11))** to be connected at $Q_0 = 10^{-1}$GeV and form a continuous graph to use henceforth.
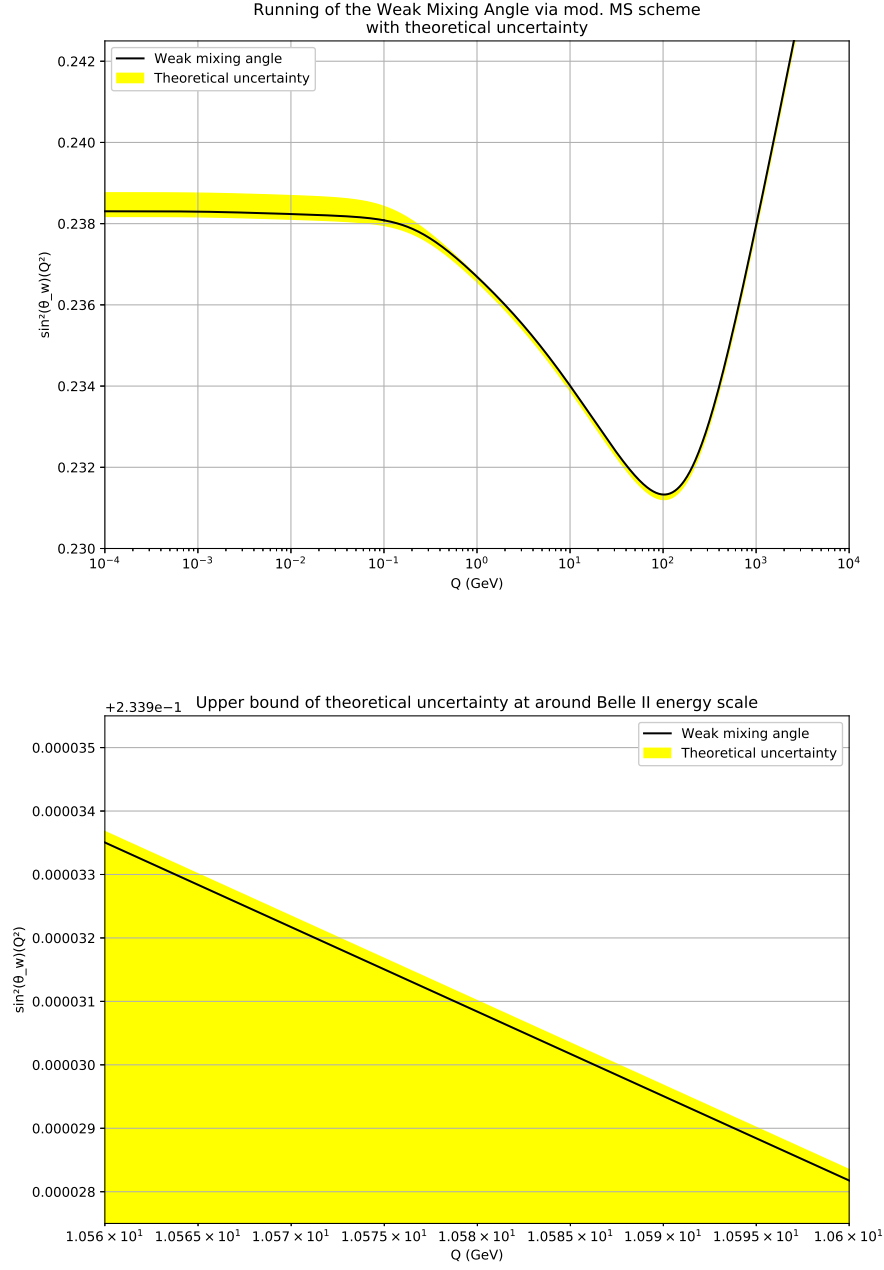
Figure 7: This is the Standard Model's running of the weak mixing angle as predicted by the $\overline{MS}$ scheme. Note how the upper bound of the theoretical uncertainty is near negligible, as compared to the lower bound.

2.4 Measuring the Weak Mixing Angle at Belle II

Now that we have an expression for weak mixing angle, let us look at how it is, and how it could be, measured at the Belle II experiment. For the purposes of this thesis, it is adequate to quote the results below (which have been modified slightly in regards to notation, to maintain consistency):

$$M_w^2 = \frac{\pi\alpha}{\sqrt{2}G_\mu s_w(1-\Delta r)} \quad (Eqn.\ 57, [2]) \tag{12}$$

$$A_{LR}^{0+1} = -\frac{s}{8M_w^2}\frac{1-s_w^2}{s_w^2}\frac{2\cos a\cos b + 6(\cos a + \cos b) + \cos 2a + \cos 2b + 8}{2\cos a\cos b + \cos 2a + \cos 2b + 8} + \Delta_{LR} \quad (Eqn.\ 66, [2]) \tag{13}$$

$$A_{FB}^{0+1} = a_l^2\frac{6s\cos a}{3+\cos^2 a}\frac{s(1+2v_l^2)-M_z^2}{(s-M_z^2)^2 + 2sv_f^2(s-M_z^2) + s^2(v_l^2 + a_l^2)} + \Delta_{FB} \quad (Eqn.\ 69, [2]) \tag{14}$$

Also, recall from (1) that:

$$\sin^2\theta_w(Q^2) = \kappa(Q^2)_{(on-shell)}s_w^2$$

where,

$s_w = \sin^2\theta_{w(on-shell)} = \ <value\ in\ (5)>$

α = Fine structure constant as measured via on-shell renormalization scheme

G_μ = Fermi constant

a_l = axial vector coupling of charged leptons = $-\frac{1}{2}$ [14]

v_l = vector coupling of leptons = $-\frac{1}{2} + 2s_w$[14][27]

$s = Q^2$; because $here$, $y \to 1$ (See table 1)

$a\ <\ \Omega\ <\ b$ is the acceptance of the detector and the angular range over which the cross-sections are integrated

A_{FB}^{0+1} and A_{LR}^{0+1} are the integrated forward-backward and left-right asymmetries respectively. They are experimentally measured by measuring the integrated relevant integrated cross-sections of the particles that hit the detector.[28]

and κ, Δr, Δ_{LR} and Δ_{FB}, are relevant one-loop radiative corrections to Born (tree-level) asymmetry and they all depend on s. Consequently, effective $\sin^2\theta_w$ and M_w change with Q^2 (or s). Therefore, by varying M_w, you can simultaneously vary the asymmetries (A_{FB}^{0+1} and A_{LR}^{0+1}), and $\sin^2\theta_w$. This way, one can obtain A_{LR} (or A_{LR}) dependence on $\sin^2\theta_w$, at measure $\sin^2\theta_w$ at any s [2]. This leads to the dependencies described in Figures 8 and 9 below:

Hence the $\sin^2\theta_w(Q^2 = 10.58^2 GeV^2)$ found from measurement can be compared to it its corresponding theoretical expression and uncertainty given in Section 2.3. A discrepancy between theoretical and experimental values, would imply the existence of phenomena beyond the Standard Model. One such example is explored in Section 3.

---

[27]In Ref. [2], one of the aspects of the Standard Model that was meant to be tested, was lepton universality. The paper distinguishes between the axial vector coupling of electrons and muons, so as to measure possible differences in it. In this thesis, lepton universality is assumed and therefore, no such distinction is made.

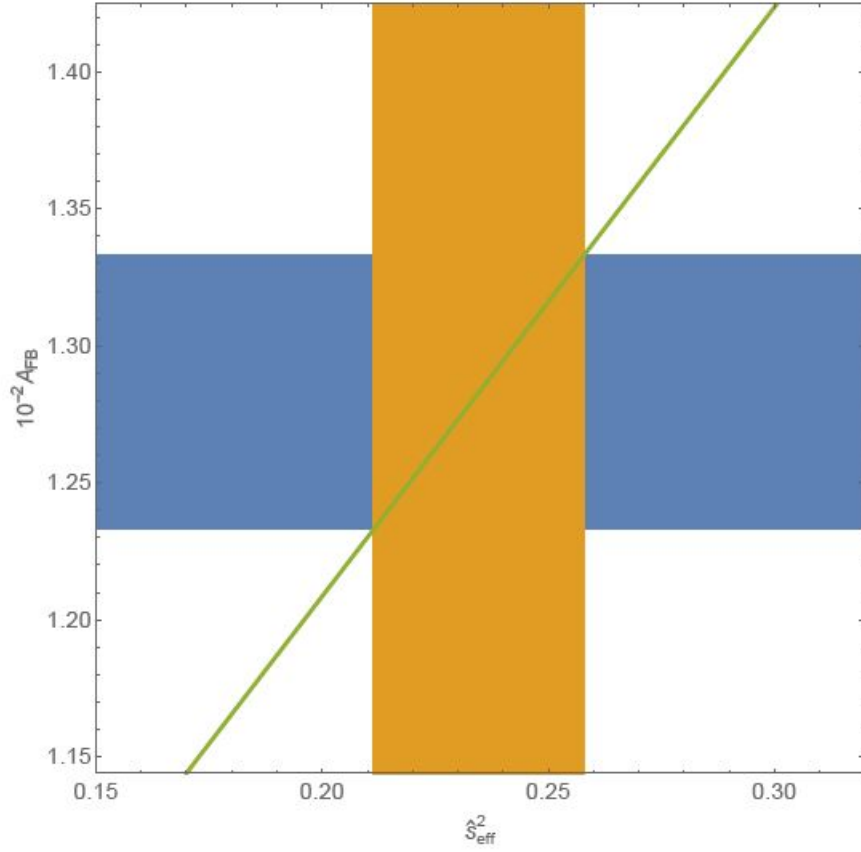[28]The exact expressions/methods for this are given in Ref. [2].

Figure 8: Forward-backward asymmetry [for $a = 10°$ & $b = 170°$] as a function of effective Weinberg mixing angle at $\sqrt{s} = 10.58$ GeV. Horizontal band shows the central value of $A_{FB}^{0+1} = 0.01283$ determined with the cut on hard-photons at 2.0 GeV. Width of the band corresponds to the 1% uncertainty on the central value of A_{FB}^{0+1}. Yields an uncertainty of 19.8% on $\sin^2 \theta_w(Q^2 = 10.58^2 GeV^2)$. (See Pg. 16-18, [2])
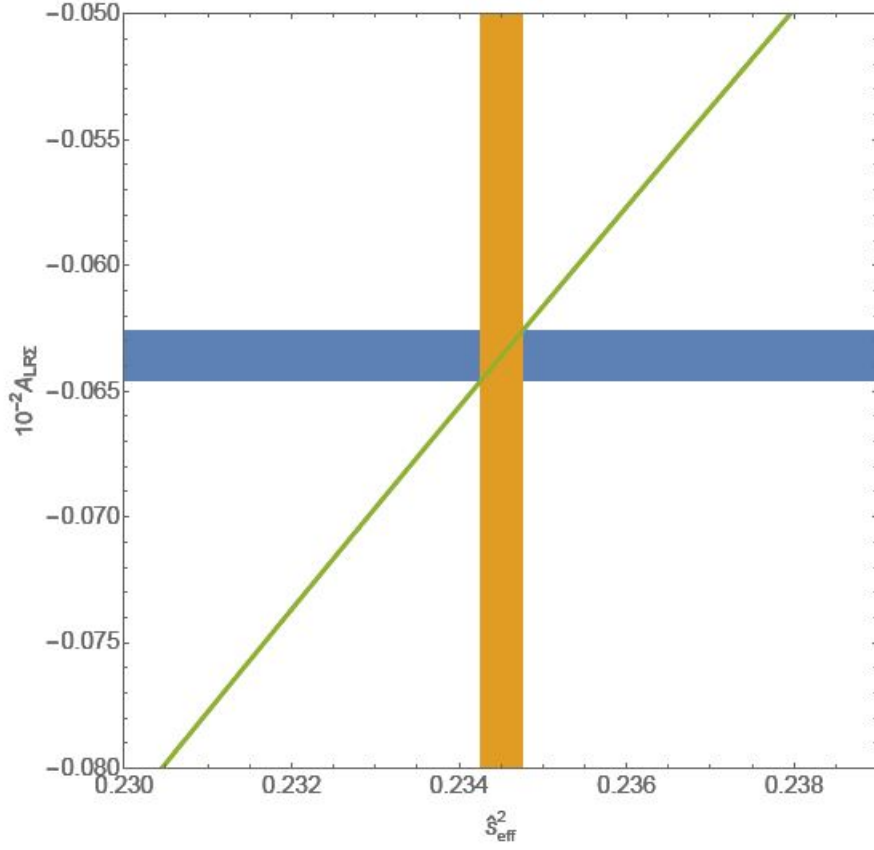
Figure 9: (Projected) Dependence of the integrated left-right asymmetry on the effective Weinberg mixing angle at $\sqrt{s} = 10.58$ GeV. Horizontal bands show the central value of $A_{LR}^{0+1} = $ -0.00063597 determined with the cut on soft-photons at 2.0 GeV. The width of the band corresponds to the ± 0.0000097 uncertainty on the central value of A_{LR}^{0+1}. Yields an uncertainty of 0.21% on $\sin^2 \theta_w (Q^2 = 10.58^2 GeV^2)$ [All figures for proposed electron beam polarization of $\sim 70\%$]. (See Pg. 16-18, [2])

3 Beyond the Standard Model: where the WIMPs come in

In recent literature, the idea of a dark Z boson (a specific type of WIMP) has grown in popularity. One of the places where it has been developed and summarized, is in Ref. [9]. The relevant result has been quoted below:

$$\sin^2 \theta_w(Q^2)_{if\ dark\ Z\ exists} \rightarrow \kappa_d(Q^2) \sin^2 \theta_w(Q^2)_{SM}$$

$$\kappa_d(Q^2) = 1 - \epsilon\delta \frac{M_Z}{M_{Z_d}} \cot \theta_w(Q^2)_{SM} \frac{M_{Z_d}^2}{Q^2 + M_{Z_d}^2} \tag{15}$$

where M_{Z_d} is the possible dark Z boson mass and ϵ & δ are model dependent parameters. In Ref. [9] these have been derived from the 2HD model. The specific origins of $\epsilon\delta$ have not been explored in this thesis - however, the possible range of values of $\sin^2 \theta_w(Q^2)_{if\ dark\ Z\ exists}$[29] have been plotted for **arbitrarily chosen** conservative estimates of $\epsilon\delta$. Please refer to Figures 10,11 &12 shown below.

As is evident from Figure 12, any expected departure from Standard Model prediction (for low-intermediate mass dark Z boson), is inaccessible without the upgrade to the SuperKEKB, allowing L-R asymmetry measurements to be made. Further research is required to obtain more precise predictions of the said dark Z boson mass, for a given $\sin^2 \theta_w(Q^2 = 10.58^2 GeV^2)$ measurement, but the point remains: at the energy scales of the Belle II experiment, the theoretical uncertainty is very low (hence favourable to us) and the required precision for possible detection is within our reach for the proposed upgrade [2]. Hence, to significantly improve our odds of detecting a WIMP, it is recommended that the electron beam of the SuperKEKB electron-positron be polarized to $\sim 70\%$ polarization.

4 Summary and Conclusion

In this thesis, we covered the theoretical origins of the Standard Model's weak mixing angle and calculated its running over the energy range $10^{-4} - 10^4$GeV. We also found the theoretical uncertainty involved in such calculations: it was advantageously low at the energy scales of the Belle II experiment. This provides strong incentive to perform precision weak mixing angle measurements at the Belle II. Finally, we calculated the possible departure from the said theoretical value of weak mixing angle, due to the presence of a dark boson (of mass $M_{Z_d} = 5, 10, 15, 20, 25, 30, 35, 40$ & 45GeV), at the energy scales of the Belle II experiment. It was found that, to detect such discrepancies from theory at the Belle II experiment, it is strongly recommended that the SuperKEKB be upgraded such that its electron beam is polarized.

—————————————x—————————————

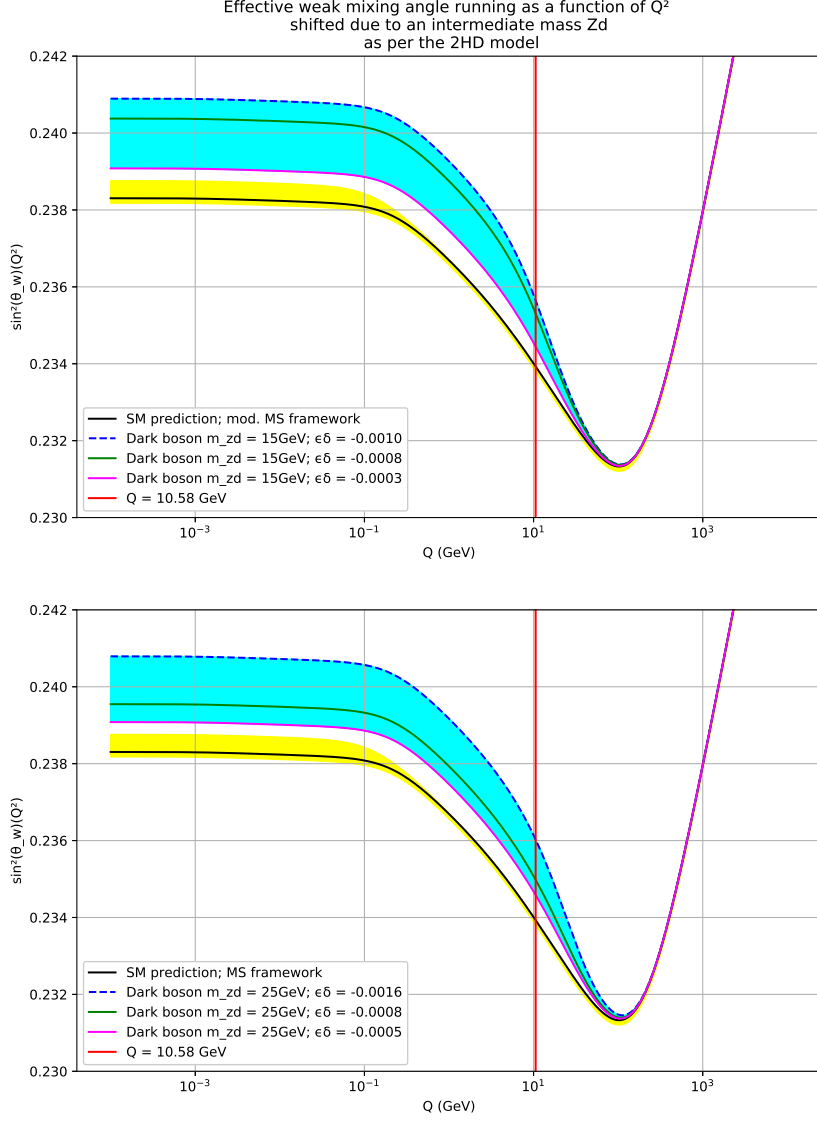
[29]Will omit [*if dark Z exists*] subscript henceforth.

Figure 10: This shows expected range for weak mixing angle, at different Q values, for probable dark Z boson masses: 15GeV and 25GeV. It attempts to replicate Fig. 3 of Ref. [9], but **additionally includes the theoretical uncertainty in weak mixing angle**. The $\epsilon\delta$ values are parameters that depend on the 2HD model, in Ref. [9]. Here, the space between the magenta line and the green middle line indicates the region which is definitely predicted by the 2HD model... while the space between magenta and blue dotted line, indicates region which are predicted by the 2HD model, but are in some tension with precision constraints.
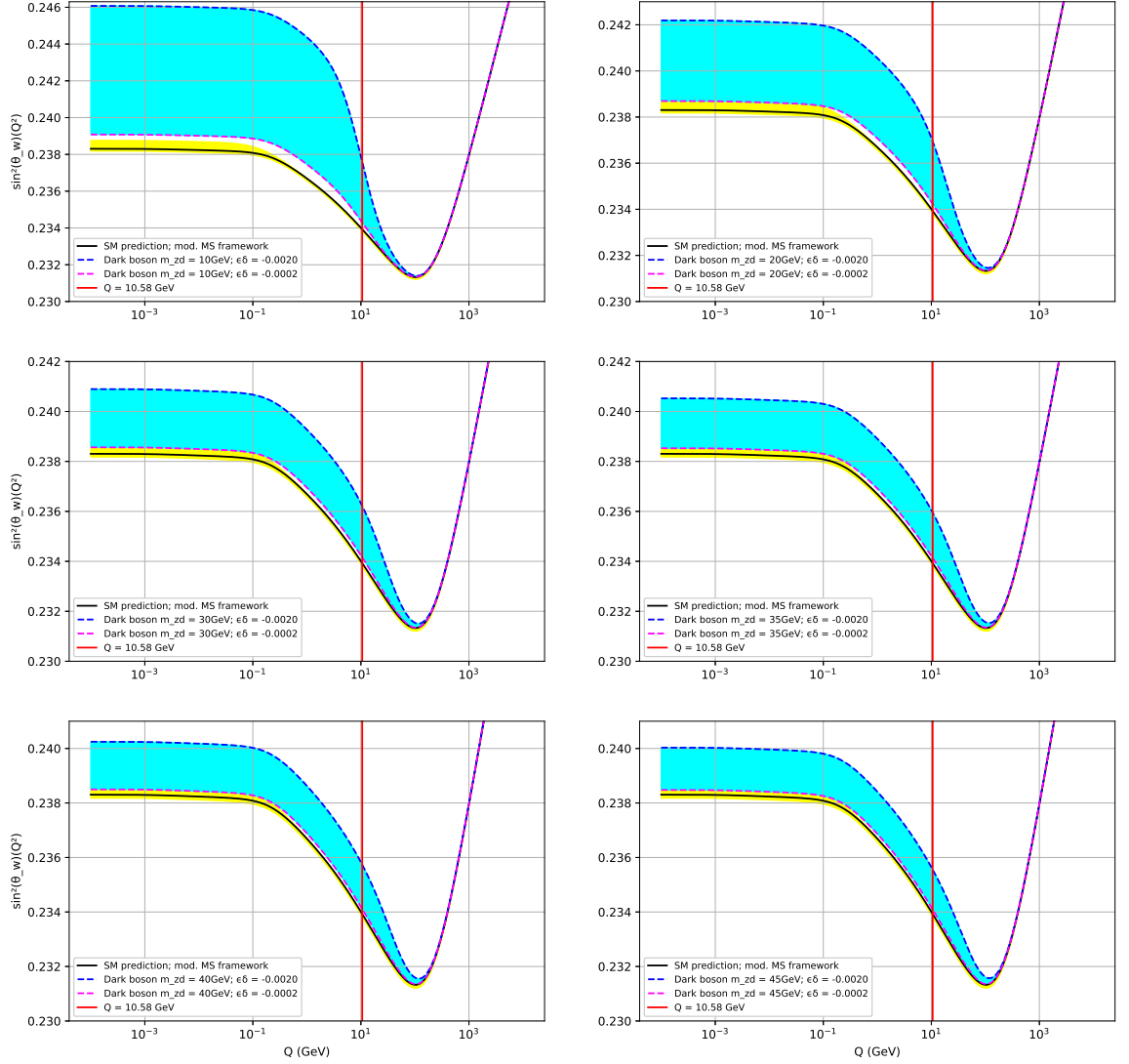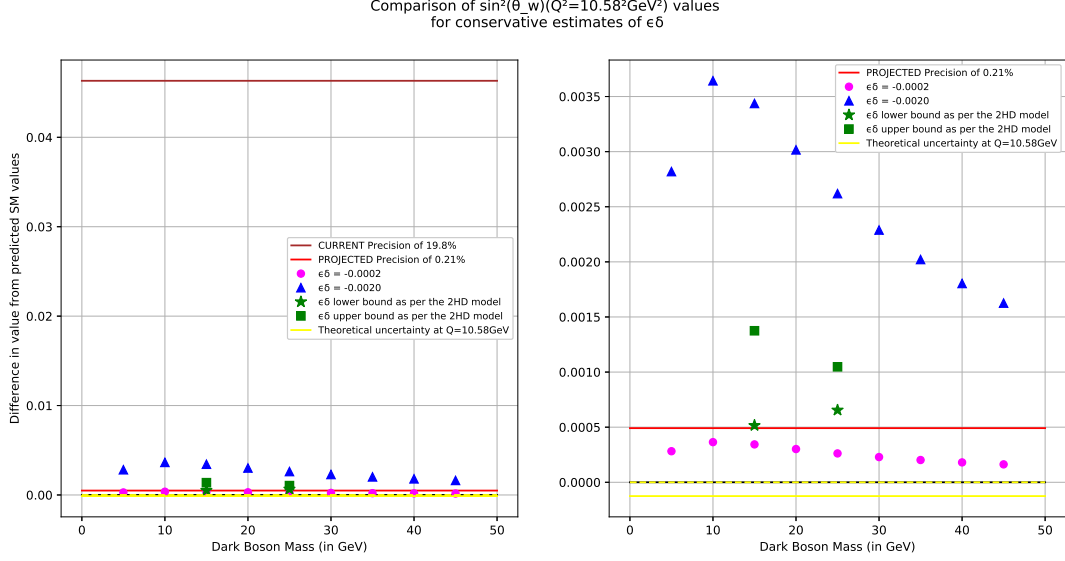
23

Figure 11: This shows expected range for weak mixing angle, at different Q values, for some probable dark Z boson masses. $\epsilon\delta$ are model dependent parameters, but we have arbitrarily chosen their values to be $0.0002 < |\epsilon\delta| < 0.0020$, to demonstrate the means by which aforementioned expected range, changed with proposed dark boson mass.

Comparison of sin²(θ_w)(Q²=10.58²GeV²) values
for conservative estimates of εδ

$sin^2\theta_w(Q^2=10.58^2GeV^2)$ = ↓					
SM Prediction →	0.2339308816306647			2HD Model constraints ↓	
Z_d boson mass ↓	εδ = -0.0002 ↓	εδ = -0.0020 ↓	εδ = -0.0003 ↓	εδ = -0.0005 ↓	εδ = -0.0008 ↓
5GeV	0.2342127797992872	0.2367498633168896			
10GeV	0.2342951618616940	0.2375736839409574			
15GeV	0.2342745855496633	0.2373679208206504	0.2344464375091625		0.235305697306659
20GeV	0.2342324981625445	0.2369470469494626			
25GeV	0.2341927910734454	0.2365499760584712		0.23458565523761638	0.234978519401788
30GeV	0.2341597623412178	0.2362196887361956			
35GeV	0.2341329965874003	0.2359520311980210			
40GeV	0.2341112720721683	0.2357347860457005			
45GeV	0.2340934597417399	0.2355566627414166			

Figure 12: This summarizes our results and also shows the precision to which weak mixing angle can be measured at SuperKEKB (at $Q = 10.58$ GeV), both at present and in the future, as a result of the proposed upgrade[1] (See Ref. [2]). Note that the dark-boson's expected range is only accessible to measurement, after the proposed upgrade.

[1]It is anticipated that the projected precision will be even higher than shown in the graph. This is because the 0.21% uncertainty was calculated using $e^+ + e^- \to \mu^+ + \mu^-$ events for $20ab^{-1}$ of data with 70% polarization. We expect that with extra measurements made from $e^+ + e^- \to e^+ + e^-$ and $e^+ + e^- \to \tau^+ + \tau^-$ events, the overall error on $\sin^2\theta_W$ will decrease substantially [25][2]

5   References

[1] Kazunori Akai, Kazuro Furukawa, and Haruyo Koiso. Superkekb collider. *Nuclear Instruments and Methods in Physics Research Section A: Accelerators, Spectrometers, Detectors and Associated Equipment*, 907:188–199, Nov 2018. `https://arxiv.org/abs/1809.01958`.

[2] A. Aleksejevs, S. Barkanova, C. Miller, J. M. Roney, and V. Zykunov. Nlo radiative corrections for forward-backward and left-right asymmetries at a b-factory, 2018.

[3] S. Boran, S. Desai, E. O. Kahya, and R. P. Woodard. Gw170817 falsifies dark matter emulators. *Physical Review D*, 97(4), Feb 2018. `https://arxiv.org/abs/1710.06168`.

[4] James Ward Brown and Ruel Vance Churchill. *Complex variables and applications*. W. Ross Mac-Donald School Resource Services Library, 2018.

[5] Hsin-Chia Cheng, Wei-Chih Huang, Xiaoyuan Huang, Ian Low, Yue-Lin Sming Tsai, and Qiang Yuan. Ams-02 positron excess and indirect detection of three-body decaying dark matter. *Journal of Cosmology and Astroparticle Physics*, 2017(03):041–041, Mar 2017. `https://arxiv.org/abs/1608.06382`.

[6] Andrzej Czarnecki and William J. Marciano. Electroweak radiative corrections to polarized moller scattering asymmetries. *Physical Review D*, 53(3):1066–1072, Feb 1996. `https://arxiv.org/abs/hep-ph/9507420`.

[7] Andrzej Czarnecki and William J. Marciano. Polarized moller scattering asymmetries. *International Journal of Modern Physics A*, 15(16):2365–2375, Jun 2000. `https://arxiv.org/abs/hep-ph/0003049`.

[8] Hooman Davoudiasl, Hye-Sung Lee, and William J. Marciano. "dark"zimplications for parity violation, rare meson decays, and higgs physics. *Physical Review D*, 85(11), Jun 2012. `https://arxiv.org/abs/1203.2947`.

[9] Hooman Davoudiasl, Hye-Sung Lee, and William J. Marciano. Low q^2 weak mixing angle measurements and rare higgs decays. *Physical Review D*, 92(5), Sep 2015. `https://arxiv.org/abs/1507.00352`.

[10] Jens Erler and Michael J. Ramsey-Musolf. Weak mixing angle at low energies. *Physical Review D*, 72(7), Oct 2005. `https://arxiv.org/abs/hep-ph/0409169`.

[11] Jens Erler and Shufang Su. The weak neutral current. *Progress in Particle and Nuclear Physics*, 71:119–149, Jul 2013. `https://arxiv.org/abs/1303.5522`.

[12] M. Tanabashi et al. (Particle Data Group). 2019 review of particle physics. *Physical Review D*, 98, 2019. `http://pdg.lbl.gov/2019/reviews/contents_sports.html`; 10. Electroweak Model and Constraints on New Physics.

[13] A. Ferroglia, G. Ossola, and A. Sirlin. The electroweak form factor $\hat{\kappa}(q^2)$ and the running of $\sin^2 \hat{\theta}_{\mathrm{w}}$. *The European Physical Journal C*, 34(2):165–171, May 2004. `https://arxiv.org/abs/hep-ph/0307200`.

[14] David J. Griffiths. *Introduction to Elementary Particles (2nd Edition)*. Wiley-VCH, 2008.

[15] Wolfgang Hollik. Electroweak theory. *Journal of Physics: Conference Series*, 53:7–43, nov 2006.

[16] G.'t Hooft. Dimensional regularization and the renormalization group. *Nuclear Physics*, B61, May 1973. Pg. 455-468.

[17] Hagen Kleinert and Verena Schulte-Frohlinde. *Critical properties of phi-4 theories*. World Scientific, 2001. See Chapter 8 and 9.

[18] K.S. Kumar, Sonny Mantry, W.J. Marciano, and P.A. Souder. Low-energy measurements of the weak mixing angle. *Annual Review of Nuclear and Particle Science*, 63(1):237–267, Oct 2013. `https://arxiv.org/abs/1302.6263`.

[19] Lancaster and Blundell. *Quantum Field Theory for the Gifted Amateur*. Oxford University Press, 2014.

[20] Joseph D. Lykken. Beyond the standard model, 2010.

[21] W. J. Marciano and A. Sirlin. Radiative corrections to atomic parity violation. *Phys. Rev. D*, 27:552–556, Feb 1983.

[22] C.Y. Prescott. Parity violation in inelastic scattering of polarized electrons. *AIP Conference Proceedings*, 1978.

[23] Ian F. Putnam. Math 212: Introduction to algebra. Chapter 3 of Course notes from titular Math 212 course, taught at the University of Victoria, BC, Canada, Dec 2017.

[24] G. Rajasekaran. Fermi and the theory of weak interactions. *Resonance*, 19(1):18–44, Jan 2014. https://arxiv.org/abs/1403.3309.

[25] J. Michael Roney. Electroweak physics with polarized electron beams in a superkekb upgrade, 2019.

[26] D. Wang, K. Pan, R. Subedi, X. Deng, Z. Ahmed, K. Allada, K. A. Aniol, D. S. Armstrong, J. Arrington, V. Bellini, and et al. Measurements of parity-violating asymmetries in electron-deuteron scattering in the nucleon resonance region. *Physical Review Letters*, 111(8), Aug 2013. https://arxiv.org/abs/1304.7741.

Glossary

abelian In regards to groups and/or (their) binary operators, it means the operator is commutative i.e. a ∘ b = b ∘ a (See Ref. [23]). Back to Pg. 2

cross-section It is a measure of the probability of a process to happen. It is typically measured in units of 'area' (usually barns or fm^2) and typically pertains to scattering processes. Back to Pg. 6

Feynman Diagram It is a quick and easy way to pictorially represent interactions permitted by the field Lagrangian, of a given theory. Every allowed interaction has its own Feynman diagrams. Quantum Field Theory is, in part, based on the principle that "every possibility does, in fact, occur" [19]. So if there are an infinite number of possibilities for a given interaction (as is the case in QED and QCD), there are an infinite number of diagrams for that interaction. Some diagrams have a higher probability i.e. contribute more to the occurrence of the interaction, than others; it is typically recommended that the cross-section of these diagrams be analyzed first. Choosing the relevant diagrams to work through, depends on the details of the theory and the effect to be observed (See Ref. [14][19]) Back to Pg. 6

Mandelstam variable There are 3 quantities that show up frequently in High-Energy Particle Physics: 's', 't' and 'u'. These are called Mandelstam variables. They make working with 4-vectors easier and more efficient. 's' and 't' are defined in table 1. $u = (p_1 - p_4)^2 = (p_3 - p_2)^2$ - same symbols as in table 1 (See Ref. [14]) Back to Pg. 6

parity Here, it refers to the eigenvalue of the Parity Operation. A Parity Operation, takes the space from $(x, y, z) \rightarrow (-x, -y, -z)$. A vector-like quantity that is symmetric under the parity operation is called a vector (examples include position $\vec{x}$ and momentum $\vec{p}$). A vector-like quantity that is anti-symmetric under the parity operation is called an axial vector/pseudo-vector (examples include angular momentum $\vec{L}$ and spin $\vec{s}$) (See Ref. [14]). Back to Pg. 1

polarization Here, polarization refers to Spin Polarization i.e. the degree to which the spin of elementary particles is aligned in a given direction [14]. Back to Pg. 2